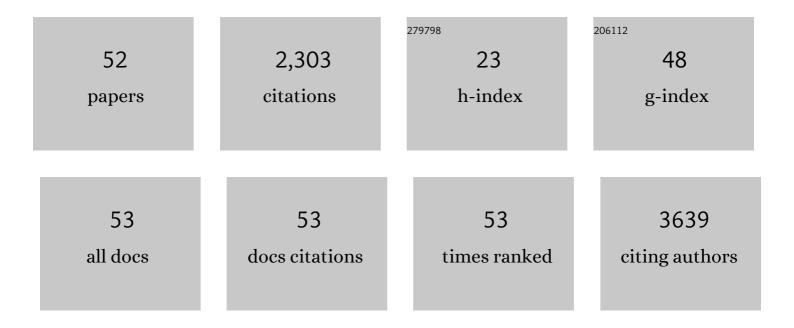
Ya-Qiong Xu

List of Publications by Year in descending order

Source: https://exaly.com/author-pdf/7862484/publications.pdf Version: 2024-02-01



Υλ-ΟιοΝς Χιι

#	Article	IF	CITATIONS
1	Half-Metallic Ferromagnetism and Structural Stability of Zincblende Phases of the Transition-Metal Chalcogenides. Physical Review Letters, 2003, 91, 037204.	7.8	321
2	Polarized photocurrent response in black phosphorus field-effect transistors. Nanoscale, 2014, 6, 8978-8983.	5.6	308
3	Controlled Multistep Purification of Single-Walled Carbon Nanotubes. Nano Letters, 2005, 5, 163-168.	9.1	130
4	Half-metallic ferromagnetism of MnBi in the zinc-blende structure. Physical Review B, 2002, 66, .	3.2	127
5	Anisotropic photocurrent response at black phosphorus–MoS ₂ p–n heterojunctions. Nanoscale, 2015, 7, 18537-18541.	5.6	118
6	High-Performance WSe ₂ Phototransistors with 2D/2D Ohmic Contacts. Nano Letters, 2018, 18, 2766-2771.	9.1	105
7	Formation of Highly Dense Aligned Ribbons and Transparent Films of Single-Walled Carbon Nanotubes Directly from Carpets. ACS Nano, 2008, 2, 1871-1878.	14.6	98
8	Vertical Array Growth of Small Diameter Single-Walled Carbon Nanotubes. Journal of the American Chemical Society, 2006, 128, 6560-6561.	13.7	93
9	Investigation of Optimal Parameters for Oxide-Assisted Growth of Vertically Aligned Single-Walled Carbon Nanotubes. Journal of Physical Chemistry C, 2009, 113, 4125-4133.	3.1	91
10	Plasmonic Hot Electron Induced Photocurrent Response at MoS ₂ –Metal Junctions. ACS Nano, 2015, 9, 5357-5363.	14.6	91
11	Dry Contact Transfer Printing of Aligned Carbon Nanotube Patterns and Characterization of Their Optical Properties for Diameter Distribution and Alignment. ACS Nano, 2010, 4, 1131-1145.	14.6	90
12	Half-metallic ferromagnetism of MnBi in zincblende phase. Physica B: Condensed Matter, 2003, 329-333, 1117-1118.	2.7	48
13	Effects of atomic hydrogen and active carbon species in 1mm vertically aligned single-walled carbon nanotube growth. Applied Physics Letters, 2006, 89, 123116.	3.3	45
14	Membrane cholesterol mediates the cellular effects of monolayer graphene substrates. Nature Communications, 2018, 9, 796.	12.8	45
15	Observation of superdiffusive phonon transport in aligned atomic chains. Nature Nanotechnology, 2021, 16, 764-768.	31.5	43
16	Electrical and Thermal Transport through Silver Nanowires and Their Contacts: Effects of Elastic Stiffening. Nano Letters, 2020, 20, 7389-7396.	9.1	40
17	Supergrowth of Nitrogen-Doped Single-Walled Carbon Nanotube Arrays: Active Species, Dopant Characterization, and Doped/Undoped Heterojunctions. ACS Nano, 2011, 5, 6925-6934.	14.6	37
18	Distinct Signatures of Electron–Phonon Coupling Observed in the Lattice Thermal Conductivity of NbSe ₃ Nanowires. Nano Letters, 2019, 19, 415-421.	9.1	37

YA-QIONG XU

#	Article	IF	CITATIONS
19	The relationship between the Young's modulus and dry etching rate of polydimethylsiloxane (PDMS). Biomedical Microdevices, 2019, 21, 26.	2.8	31
20	Dual-modality photothermal optical coherence tomography and magnetic-resonance imaging of carbon nanotubes. Optics Letters, 2012, 37, 872.	3.3	30
21	Visualizing Light Scattering in Silicon Waveguides with Black Phosphorus Photodetectors. Advanced Materials, 2016, 28, 7162-7166.	21.0	29
22	Alignment dependence of one-dimensional electronic hopping transport observed in films of highly aligned, ultralong single-walled carbon nanotubes. Applied Physics Letters, 2009, 94, .	3.3	23
23	Near-infrared optical transitions in PdSe ₂ phototransistors. Nanoscale, 2019, 11, 14410-14416.	5.6	23
24	Gateâ€īunable Photoresponse Time in Black Phosphorus–MoS ₂ Heterojunctions. Advanced Optical Materials, 2019, 7, 1800832.	7.3	23
25	Bending and Twisting of Suspended Single-Walled Carbon Nanotubes in Solution. Nano Letters, 2009, 9, 1609-1614.	9.1	21
26	Ultrafast Photocurrent Response and High Detectivity in Two-Dimensional MoSe ₂ -based Heterojunctions. ACS Applied Materials & Interfaces, 2020, 12, 46476-46482.	8.0	21
27	Impact of Graphene on the Efficacy of Neuron Culture Substrates. Advanced Healthcare Materials, 2018, 7, e1701290.	7.6	20
28	Reversible photo-induced doping in WSe ₂ field effect transistors. Nanoscale, 2019, 11, 7358-7363.	5.6	20
29	Ultrathin Single-Walled Carbon Nanotube Network Framed Graphene Hybrids. ACS Applied Materials & Interfaces, 2015, 7, 5233-5238.	8.0	19
30	Photonic Structure-Integrated Two-Dimensional Material Optoelectronics. Electronics (Switzerland), 2016, 5, 93.	3.1	19
31	Effect of Competitive Surface Functionalization on Dual-Modality Fluorescence and Magnetic Resonance Imaging of Single-Walled Carbon Nanotubes. Journal of Physical Chemistry C, 2012, 116, 16319-16324.	3.1	14
32	Probing electrical signals in the retina via graphene-integrated microfluidic platforms. Nanoscale, 2016, 8, 19043-19049.	5.6	14
33	Ultrasensitive Graphene Optoelectronic Probes for Recording Electrical Activities of Individual Synapses. Nano Letters, 2018, 18, 5702-5708.	9.1	13
34	Curling graphene ribbons through thermal annealing. Applied Physics Letters, 2013, 103, 183103.	3.3	9
35	Thermal and optical properties of freestanding flat and stacked single-layer graphene in aqueous media. Applied Physics Letters, 2014, 104, .	3.3	9
36	Probing photoresponse of aligned single-walled carbon nanotube doped ultrathin MoS ₂ . Nanotechnology, 2018, 29, 345205.	2.6	9

YA-QIONG XU

#	Article	IF	CITATIONS
37	Tunneling Effects in Crossed Ta ₂ Pt ₃ Se ₈ –Ta ₂ Pd ₃ Se ₈ Nanowire Junctions: Implications for Anisotropic Photodetectors. ACS Applied Nano Materials, 2021, 4, 1817-1824.	5.0	9
38	Single-Walled Carbon Nanotube-Mediated Small Interfering RNA Delivery for Gastrin-Releasing Peptide Receptor Silencing in Human Neuroblastoma. Methods in Molecular Biology, 2013, 1026, 137-147.	0.9	8
39	Enhanced photoresponse in curled graphene ribbons. Nanoscale, 2013, 5, 12206.	5.6	8
40	Direct Measurement of π Coupling at the Single-Molecule Level using a Carbon Nanotube Force Sensor. Nano Letters, 2018, 18, 7883-7888.	9.1	8
41	Enhanced photocurrent response speed in charge-density-wave phase of TiSe ₂ -metal junctions. Nanoscale, 2021, 13, 11836-11843.	5.6	8
42	Atomic-ensemble-based quantum repeater against general polarization and phase noise. Physical Review A, 2011, 84, .	2.5	6
43	Magneto-fluorescent carbon nanotube-mediated siRNA for gastrin-releasing peptide receptor silencing in neuroblastoma. RSC Advances, 2013, 3, 4544.	3.6	5
44	Net negative contributions of free electrons to the thermal conductivity of NbSe ₃ nanowires. Physical Chemistry Chemical Physics, 2020, 22, 21131-21138.	2.8	4
45	Formation mechanism of adatom islands on fcc (111) substrates. Journal Physics D: Applied Physics, 2001, 34, 1137-1142.	2.8	3
46	Growth of Single-Walled Carbon Nanotubes on a Nanorough Surface. Journal of Physical Chemistry C, 2007, 111, 9142-9145.	3.1	3
47	In situ monitoring of electrical and optoelectronic properties of suspended graphene ribbons during laser-induced morphological changes. Nanoscale Advances, 2020, 2, 4034-4040.	4.6	3
48	Probing Light-Stimulated Activities in the Retina via Transparent Graphene Electrodes. ACS Applied Bio Materials, 2022, 5, 305-312.	4.6	2
49	Theoretical study of dielectronic recombination between electrons and heliumlike carbon ions. Physical Review A, 2000, 62, .	2.5	1
50	Relativistic Calculation of Dielectronic Recombination on the C 4+ Ground State. Chinese Physics Letters, 2001, 18, 761-763.	3.3	1
51	Controlling the growth morphology of carbon nanotubes: from suspended bridges to upright forests. Nanoscale, 2012, 4, 1682.	5.6	1
52	Optical Momentum Alignment Effect in WSe 2 Phototransistor. Advanced Optical Materials, 2021, 9, 2002243.	7.3	0